A&A 427, 345–351 (2004)
DOI: 10.1051/0004-6361:20041151

Astronomy & Astrophysics

The sensitivity of the C I 538.0 nm Fe I 537.9 nm and Ti II 538.1 nm lines to solar active regions

V. Penza[1], B. Caccin[2,†⋆], and D. Del Moro[2]

[1] INAF - Osservatorio astronomico di Roma , Via Frascati 33, 00040, Monte Porzio Catone, Italia
e-mail: penza@mporzio.astro.it
[2] Dipartimento di Fisica, Università di Roma "Tor Vergata", Via della Ricerca Scientifica 1, 00133 Roma, Italia

Received 23 April 2004 / Accepted 5 July 2004

Abstract. Using spectroscopy to probe stellar global parameters, such as effective temperature, is much exploited in the literature. In the solar case it can be used as an indicator of magnetic cycle variations. In this work we study the sensitivity to bright active regions of three photospheric lines (Fe I 537.9 nm, C I 538.0 nm and Ti II 538.1 nm), which have been monitored on the sun for more than twenty years.
In our analysis we compare our experimental results, from observations with the THEMIS telescope, with theoretical results, obtained by spectral synthesis with FAL semi empirical models (Fontenla et al. 1999, ApJ, 518, 480). We demonstrate the inappropriateness of using these lines (full disk integrated) as indicators of quiet sun irradiance modifications without considering their intrinsic variations due to active regions. Instead, their different sensitivity to the presence of active regions can be exploited in order to discriminate the background quiet sun variations from the magnetic region contributions.

Key words. Sun: atmosphere – Sun: activity – Sun: faculae, plages – radiative transfer

1. Introduction

The use of spectroscopic diagnostics for the determination of stellar global parameters, for example $T_{\rm eff}$ or radius, has a place in the literature (Gray 1992; Gray & Johanson 1991; Ulrich & Bertello 1995). In the solar case, spectral diagnostics play a role as cyclic variation indicators. It is well-known that the total solar irradiance (TSI, i.e. the energetic flux emitted by the Sun, integrated over the whole wavelength range and measured at 1 AU) varies by about 0.10–0.15% in phase with the magnetic activity (Hoyt et al. 1992; Fröhlich 1994). The irradiance variations show a strong wavelength dependence, with a dramatic increase towards shorter wavelengths; indeed percentage variations at UV and shorter wavelengths exceed those in the visible by as much as two orders of magnitude. This spectral dependence can be exploited in order to distinguish the different mechanisms contributing to the TSI variation. In fact, while there is no doubt that the largest part of the TSI variations on the shorter time-scales are associated with the spatial and temporal distribution of the active regions (Willson et al. 1981; Sofia et al. 1982; Foukal & Lean 1986; Chapman et al. 1986), the origin of the irradiance variations over magnetic cycle time-scales is still an open topic.

Most of the literature on solar variability assumes that faculae and enhancement of quiet magnetic network, together with sunspot darkening, explain all of the solar variability (Foukal & Lean 1988; Willson & Hudson 1991; Krivova et al. 2003). However, the variation of the background, on which these features are superposed, deserves more investigation (Lydon et al. 1996; Penza et al. 2003). It is reasonable that the whole solar structure varies as a consequence of global modifications due to variations of the magnetic field both in the solar interior (where the dynamo process operates) and at the surface (where the activity modifies the boundary conditions).

To shed light on this complex scenario, Gray & Livingston (1997a,b, G&L henceforth) used a calibration of the variations of three line depths (Fe I 537.958 nm, C I 538.032 nm and Ti II 538.103 nm) with the $T_{\rm eff}$, to infer the background contribution to the TSI variations. It has been shown that such a calibration was affected by a systematic error (Caccin et al. 2002) and that, by using the correct calibration, a result incompatible with observations is obtained. Moreover, the same G&L data concerning the individual lines cannot be reproduced by $T_{\rm eff}$ variation alone, thus supporting the idea that something else is occurring. Indeed, these lines should respond quite differently to $T_{\rm eff}$ changes (see following paragraph); on the contrary, all of the line depths observed by G&L vary concurrently. We note that it would be impossible to ascribe this trend to some multiplicative instrumental effect (e.g. scattered light, as

⋆ We regret to note that, during the editorial revision, Bruno Caccin passed on June 19, 2004.

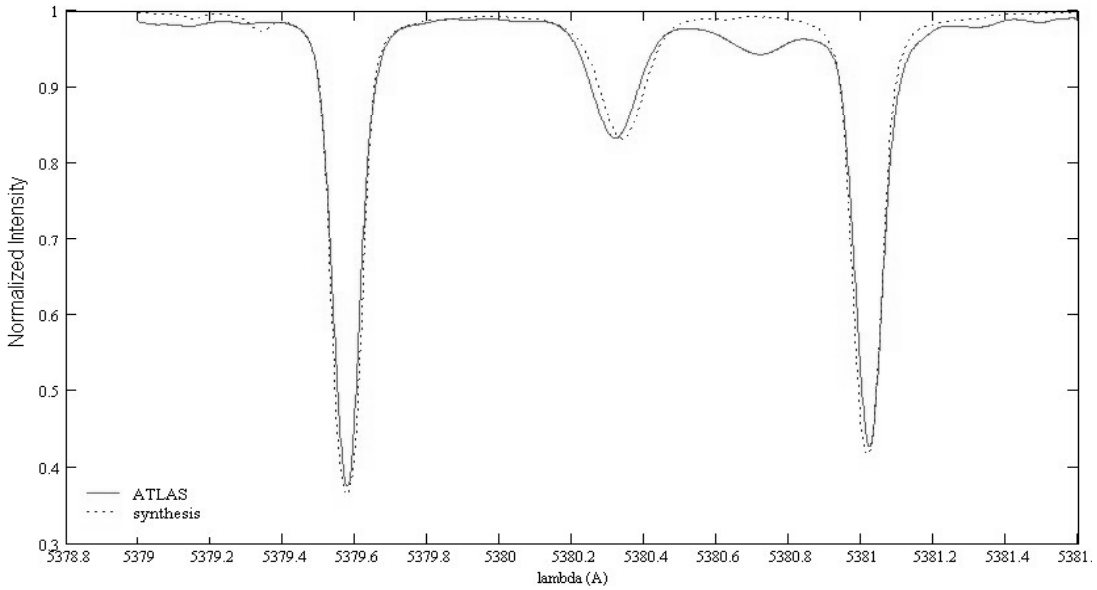

Fig. 1. Theoretical synthesis of the C I 538.032 nm, Fe I 537.958 nm and Ti II 538.103 nm lines, compared with atlas profiles.

suggested by G&L) because there is not a unique correction factor for all of the three lines (Gray & Livingston 1997c); moreover it is improbable that an instrumental effect will vary with the cycle.

In this work we try to account for such cyclic line behavior. We judge it likely that Fe I, C I and Ti II are affected by the presence of active regions (whereas G&L ruled this out on the basis of a declared absence of a rotation signal). We study the active region effects on these lines and our analysis shows that the presence of active regions significantly modifies them.

We compare theoretical results, obtained by spectral synthesis with FAL semiempirical models (Fontenla et al. 1999), with experimental ones, obtained from THEMIS data.

2. Lines characteristics in quiet average sun

The theoretical synthesis of the lines under study (Fe I 537.958 nm, C I 538.032 nm and Ti II 538.103 nm) is obtained by using modC of the FAL models (Fontenla et al. 1999) as typical of a quiet average sun. In Fig. 1 the theoretical synthesis is compared with the atlas data (Kurucz et al. 1985).

This spectrum synthesis was computed, via the SPECTRUM program by R.O. Gray (1994). Details of this program are available at `http://www.phys.appstate.edu/spectrum/spectrum.html`; here we recall only that SPECTRUM computes synthetic spectra under LTE assumptions and considers each line as pure absorption (i.e. the source function is the Planck function). In order to avoid the inconsistency of LTE treatment in the presence of semiempirical models, where chromospheric temperature rises, we used modified models (Unruh et al. 1999; Penza et al. 2004), where the temperature structure is truncated at about the temperature minimum and then extrapolated down to lower temperatures, with a trend similar to Kurucz's models (Kurucz 1994).

We have checked that this modification does not significantly alter the spectrum and, in particular, it does not affect the intensity ratios between the models.

Table 1. Line parameters used for the calculation of line profiles. ζ is a term multiplying the Unsöld value of γ in the Lorentz part of the absorption profile, while ξ is the usual microturbulence term. The values of $\lg(gf)$, ζ and ξ are chosen to optimize the comparison with atlas data.

Line	$\chi_{\rm ion}$ (eV)	$\chi_{\rm ex}$ (eV)	$\lg(gf)$	ζ	ξ (km s^{-1})
CI 538.032 nm	11.26	7.680	−1.64	7.0	1.5
FeI 537.958 nm	7.87	3.695	−1.58	5.5	1.5
TiII 538.103 nm	13.58	1.566	−2.10	10	1.5

The line parameters that we use to optimize the comparison with the atlas are shown in Table 1.

These three lines are characterized by rather dissimilar excitation potentials (Table 1), therefore they are differently affected by temperature changes (in particular C deepens with increasing $T_{\rm eff}$, Fe becomes shallower and Ti does not vary) and their cores are formed in different atmospheric layers, so they are influenced by perturbations localized at diverse depths. Such behavior is made clear by studying the absolute intensity Response Function, RF_λ (Caccin 1977), and the normalized intensity Response Function, $RF_{\rm norm}$, which is given by:

$$RF_{\rm norm} = \frac{RF_\lambda - RF_{\rm c} \cdot I_{\rm norm}}{I_{\rm c}}, \qquad (1)$$

where $RF_{\rm c}$ and $I_{\rm c}$ are the continuum Response Function and continuum intensity, respectively, and $I_{\rm norm}$ is the spectral intensity normalized to the continuum.

The velocity and temperature RF_λ in the line cores (Fig. 2), computed at constant pressure, accounts for the different responses to perturbations localized at diverse depths, while the temperature $RF_{\rm norm}$ (Fig. 3) accounts for the behavior with temperature variations. The different maxima positions in RF_λs lead to opposite signs in $RF_{\rm norm}$s (Fig. 3). In particular, in

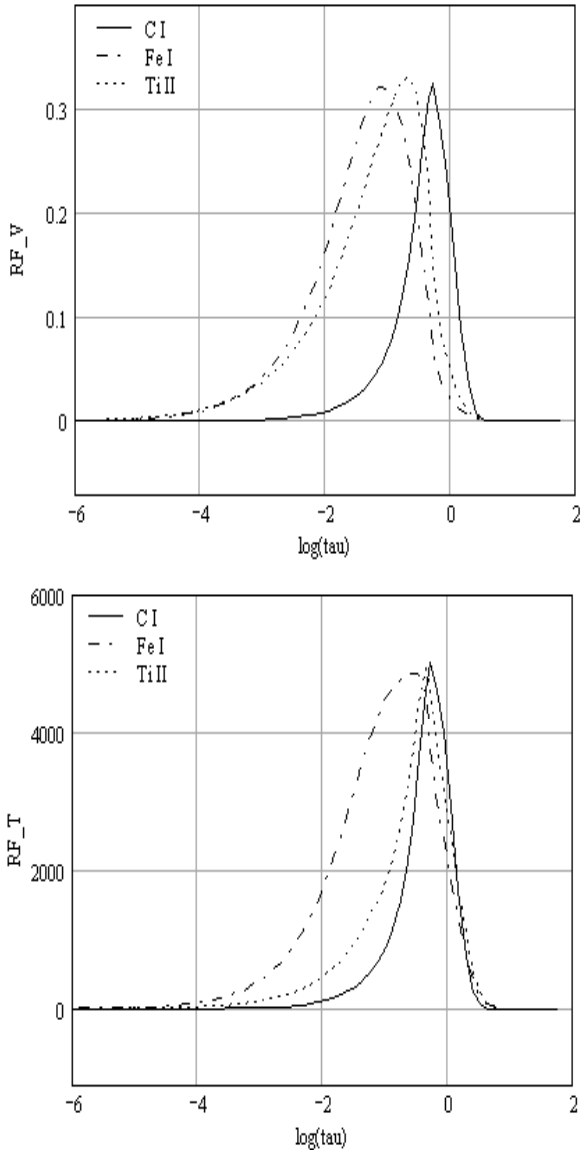

Fig. 2. Velocity (*top*) and temperature (*down*) RF_λs for our three lines. The RF_λs are arbitrarily rescaled in order to represent the functions in one plot.

the C I case $RF_{\rm norm}$ is negative everywhere, in the Fe I case the area subtended by the positive part is larger than the negative one and for the Ti II case the negative area compensates almost perfectly the positive one, making this line insensitive to temperature variations.

3. Effects of the bright active regions

3.1. Results of the models

In order to quantify the theoretical sensitivity of the three G&L lines to the presence of faculae and network, we have calculated their profile by using the bright FAL models (modE, modF, modH and modP).

A short description of the FAL models is reported in Table 2; their capability to reproduce active region characteristics has been tested in a previous work (Penza et al. 2004).

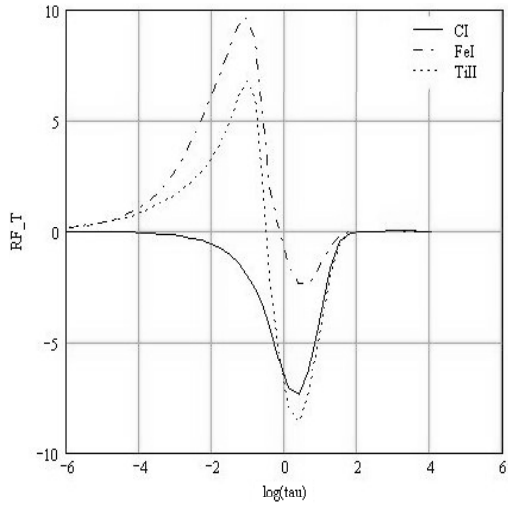

Fig. 3. Temperature $RF_{\rm norm}$s for our three lines.

Table 2. FAL model descriptions, as in Fontenla et al. (1999).

Model	Description
ModA	Faint supergranule cell, interior
ModC	Average supergranule cell interior
ModE	Average network
ModF	Bright network/Faint plage
ModH	Average plage
ModP	Bright plage
ModS	Sunspot umbra

The results of our investigation are shown in Fig. 4 and summarized in Table 3. The microturbulence value for these calculations is kept constant for all the models and the lines are considered insensitive to the magnetic field. This last assumption is justified by the rather small Landé factors ($g_{\rm Fe} = 1.096$, $g_{\rm C} \simeq 1$, $g_{\rm Ti} = 0.922$).

Two out of three lines (Fe and Ti) show a clear trend with active region type: they become weaker with increasing region brightness, suggesting that the most of the effect measured by G&L was due to active region modulation. The behavior of the C line, instead, is more ambiguous: it does not vary greatly and does not have a monotonic trend, the result being slightly deeper in modE and modF, unchanged in modH, and shallower in modP.

We stress that this theoretical synthesis seems to refute the presumed insensivity of these lines. Such a result could be guessed at by analyzing the RF_λs plotted in Fig. 2, as it is evident that the layers contributing to the Fe and Ti line formation extend from the photosphere to the base of the chromosphere.

3.2. Experimental data

The dataset used was acquired at the THEMIS telescope (Teide Observatory, Tenerife) on July 6, 2003 (from 7.05 to 9.07 UT) and July 7, 2003 (from 14.09 to 16.40 UT). It consists of a broadband (4 nm *FWHM* around 557 nm, 40 ms integration time) and a monochromatic (2.1 pm *FWHM*, 500 ms integration time) image series (0.12 arcsec/pixel resolution),

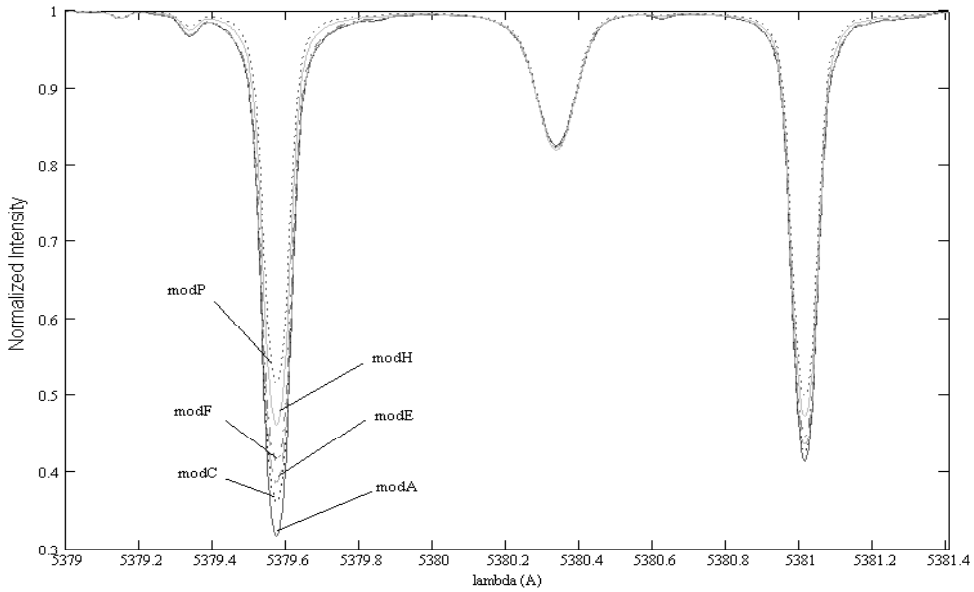

Fig. 4. Line profiles of C I, Fe I and Ti II for different active region models.

Table 3. The line depths and adjacent continuum flux for FAL models. The continuum flux unit is 10^6 erg s^{-1} cm^{-2}.

Model	D(Fe)	D(C)	D(Ti)	I_c
ModA	0.662	0.166	0.586	3.044
ModC	0.635	0.167	0.583	3.052
ModE	0.617	0.168	0.578	3.063
ModF	0.592	0.171	0.569	3.087
ModH	0.522	0.167	0.535	3.213
ModP	0.453	0.156	0.497	3.312

obtained in the IPM (Italian Panoramic Monochromator) observing mode (Cavallini 1998). A square frame (30×30 arcsec^2, 256 × 256 pixel^2) of the solar surface at the disk center, containing both quiet and bright regions, was imaged at different spectral positions along the profiles of Fe I 537.959 nm ($\Delta\lambda = 0, \pm2, \pm4.0, \pm6.0, \pm8$ pm), C I 538.032 nm ($\Delta\lambda = 0, \pm2.5, \pm5.0, \pm7.5, -10$ pm, continuum), Ti II 538.102 ($\Delta\lambda = 0, \pm2, \pm4.0, \pm6.0, \pm8$ pm) and at fixed position in the red wing of Mg I 518.740 nm. A broadband counterpart was acquired simultaneously with each monochromatic image. The July 6 dataset consists of 50 complete spectral scans, while the July 7 dataset consists of 54 complete spectral scans.

The images were corrected for dark current and flat field, then recentered and corrected for atmospheric transparency variations.

To identify the "facular" zone (FZ) in all the frames, we define as "faculae" the regions complying with this threshold criterion in Mg images:

$$I_{\rm fac} \geq I_{\rm mean} + \alpha\sigma \tag{2}$$

where $I_{\rm mean}$ and σ are Mg image mean intensity and corresponding standard deviation, respectively, and α is the threshold parameter; we chose $\alpha = 0.9$, 1.2 and 1.5, thus obtaining three "faculae" definitions (FZ_1,FZ_2, FZ_3, respectively). The higher the α the brighter the selected facular region.

The quiet region (QZ) was determined by the formula:

$$I_{\rm mean} - \beta\sigma \leq I_{\rm quiet} \leq I_{\rm mean} + \beta\sigma \tag{3}$$

where β was fixed to 0.6.

Such α and β values were chosen to separate QZ from FZ_1, while retaining a sufficiently high statistical stability for FZ_3 and including intrinsic quiet sun fluctuations in QZ. A spatial average was performed by computing the mean intensities of QZ and FZ_i, and then a temporal average was performed by computing the mean of these values using the 54 monochromatic images at the same wavelength.

The experimental line profiles, from which the central depth values were computed, were obtained via a parametric fit of the averaged spectral values with a Voigt function:

$$H(\lambda, \lambda_0, \Delta\lambda_D, \Gamma, A, B) = B + A\frac{a}{\pi}\int_{-\infty}^{+\infty}\frac{{\rm e}^{-y^2}}{a^2 + (a-y)^2}\,{\rm d}z, \tag{4}$$

where

$$a(\Gamma, \Delta\lambda_D) = \frac{\Gamma\lambda_0^2}{4\pi\Delta\lambda_D c}, \tag{5}$$

and

$$u(\lambda, \lambda_0, \Delta\lambda_D) = \frac{\lambda - \lambda_0}{\Delta\lambda_D}. \tag{6}$$

The line depth percent differences obtained by the fits are reported in Table 4. In order to have an immediate comparison with theoretical synthesis, the model results of Table 3 are reported also in Table 4 in the same percent form. An example of a spectrum fit is given in Fig. 5.

4. Discussion and conclusions

Theoretical synthesis through the FAL models seems to reproduce, both qualitatively and quantitatively, the behavior of Fe

Table 4. Line-depth percent differences between bright zones (selected with three different threshold values) and the neighboring quiet zone, as obtained from THEMIS data analysis. We report as errors the propagation of experimental errors since the fit error is always much smaller.

LINE	Theoretical				Experimental		
	δ(ModE)	δ(ModF)	δ(ModH)	δ(ModP)	FZ_1	FZ_2	FZ_3
Fe I(July6)	−2.8%	−6.8%	−17.8%	−28.7%	−2.2 ± 0.3%	−4.7 ± 0.6%	−6.6 ± 0.8%
Fe I(July7)	−2.8%	−6.8%	−17.8%	−28.7%	−6.9 ± 0.8%	−8 ± 1%	−4.2 ± 0.5%
C I(July6)	+0.6%	+2.4%	+0%	−6.6%	−1.9 ± 0.1%	−2.8 ± 0.1%	−4.2 ± 0.2%
C I(July7)	+0.6%	+2.4%	+0%	−6.6%	+4.9 ± 0.3%	+4.7 ± 0.2%	+11.1 ± 0.6%
Ti II(July6)	−0.9%	−2.4%	−8.2%	−14.8%	−0.50 ± 0.08%	−5.6 ± 0.9%	−4.2 ± 0.7%
Ti II(July7)	−0.9%	−2.4%	−8.2%	−14.8%	−0.20 ± 0.04%	−0.3 ± 0.05%	−7 ± 1%

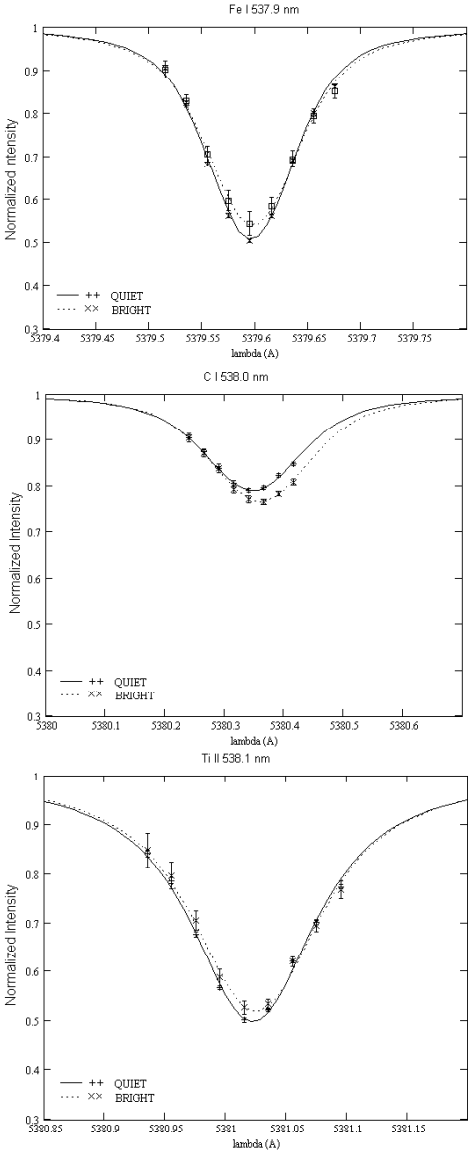

Fig. 5. An example of the mean line profiles of Fe I, C I and Ti II as best fit of the spectral positions measured at the THEMIS telescope in July 6, 2003. For the three lines the profile in the quiet region, compared with that in bright region (where the threshold is $\alpha = 1.5$), is reported. Each position represents the mean of single spectral images with the associated error, given by the corresponding standard deviation.

and Ti lines in active regions. Moreover, we stress that we are comparing temporally and spatially localized observations with models aimed to reproduce *average* behavior.

In particular, by analyzing the results in Table 4, we note that the facula/quiet contrasts for Fe I are bracketed by modE and modF, while for Ti II they are bracketed by modE and modH. In general, we can conclude that these lines, in bright active regions, are systematically shallower. An obvious corollary is the substantial sensitivity of these lines to active region presence.

It is more challenging to draw conclusions concerning the C line, which does not present an unequivocal trend: the theoretical synthesis implies a shallower line for modE and modF, a deeper line for modP and a practically unaltered depth line for modH, with respect to modC. Also the experimental data show a strange behavior, since we obtain opposite results for two observational days and it is not possible to find two models embracing the obtained differences or an analogy of the FZ behavior within the theoretical models. In particular, the only model (modP) producing a negative contrast provides a value too large, while those with positive contrast provide a value too small with respect to experimental results.

In addition, the sign of the experimental results of the contrast facula/quiet does not depend on the threshold value α, but, possibly, on intrinsic facula structure.

It seems unlikely that we could recover, through a threshold modification alone, a direct correspondence between theoretical models and observed faculae. By increasing α, we do not select faculae corresponding to a brighter model, but it is probable that we are "cutting" the facula at higher layers, i.e. we are moving along the same model at higher temperature. The passage from one model to another is linked to an intrinsic property of the faculae, e.g. the flux tube density, which is not reproducible by α modification.

The C line hides some "peculiarity", both experimentally, since it is very weak and blended in the red wing with a telluric line (H_2O), and theoretically due to FAL model constraints. The temperature structure of FAL models has been constructed by imposing the same value close to $\log(\tau) = 0$ for all of them, to reproduce experimental data (in particular in the IR). Such constraints affect the layers corresponding to the C line formation. Penza et al. (2004) showed that the brightest facular models (modH and modP) could need slight modifications in

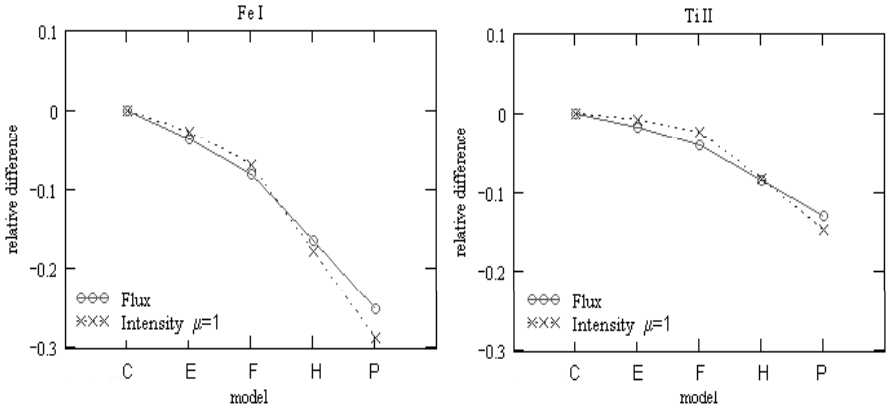

Fig. 6. Relative differences between the Fe I (*left*) and Ti II (*right*) line depths computed in active regions (models from modE to modP) and in quiet sun (modC), both for intensity at disk center and for disk-integrated flux.

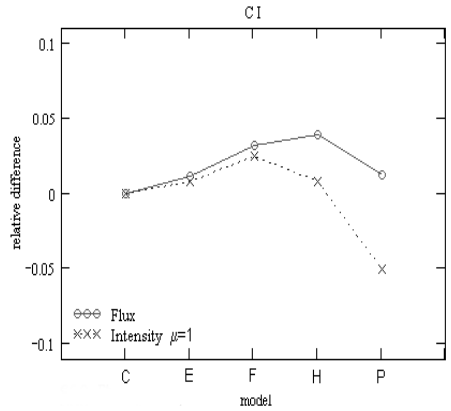

Fig. 7. Relative differences between the C I line depths computed in active regions (models from modE to modP) and in quiet sun (modC), both for intensity at disk center and for disk-integrated flux.

the deeper layers in order to better reproduce the contrast of the Rome PSPT (Precision Solar Photometric Telescope) red band (607.1 ± 0.5 nm). Fontenla et al. (2004) acknowledged that "*modeling of solar spectra irradiance [...] has to be revised to match the new observations*".

Our results, concerning Fe and Ti lines, imply that at least a part of the cyclic observed variation in these lines was due to the cyclic active region modulation. It is possible to suggest an explanation about the declared absence of a rotation signal in the G&L results: their data have an unfortunate monthly sampling, that probably masked any rotation modulation. Our results concern the line behaviors at the disk center, while the G&L data are at full disk. What they observed is the composite flux from different regions (and therefore different models), weighted by corresponding coverage factors. By supposing that these factors do not depend on disk position, the full disk flux can be written as:

$$F_{\rm tot}(\lambda) = \sum_i \alpha_i F_i(\lambda), \qquad (7)$$

where $F_i(\lambda)$ and α_i are the flux and the coverage factor of the ith model, respectively. We compared the line depth relative differences computed at the disk center with those full disk integrated, for the three lines. For Fe and Ti we found very small differences (Fig. 6).

The absence of a monotonic behavior for the C line, both in observations and theoretical models, prevent us from stating that the C modulation in G&L data stems only from active regions. Moreover, disk-integrated C lines computed in active regions are always *deeper* than in the quiet sun, i.e. the C flux does not change sign with the models (Fig. 7). Therefore, the C flux cycle modulation – if it depended on active regions only – would be in antiphase with Fe and Ti. Since C flux reported in G&L is in phase with Fe and Ti, another cause is required to account for the observations.

The behavior of the C depth in active regions at disk center (i.e., the alternate sign of their relative differences with respect to the quiet sun) could also account for the results of Livingston & Wallace (2003). Livingston & Wallace state that line intensity measurements (at disk center) of C 538.0 and C 538.0/Fe 537.9 equivalent widths do not show a cyclic modulation. Indeed, unresolved magnetic features in their field of view could have led to the cancellation of a possible C modulation.

We can speculate about a possible explanation of the cyclic behavior of the G&L full-disk data. It could derive from a modification of the center-limb variation (CLV) of the line depth, different from the CLV in the continuum. Alternatively, it could derive from a change of active region intrinsic properties (i.e., filling-factor). More details about line behavior reconstruction along the cycle will be gives in a forthcoming paper.

Our results imply that these lines should not be used as indicators of quiet sun irradiance variation, without considering their intrinsic variation due to active region modulation. Instead, by exploiting their different sensitivities, they could be used to discriminate background variations from magnetic region contributions.

Acknowledgements. The authors are indebted to R. Falciani for profit indications. They are grateful to F. Berrilli and M. Centrone for fruitful discussions. They thank the referee, W. Livinston, for the useful comments. The THEMIS is operated on the island of Tenerife by CNRS and CNR in the Spanish Observatorio del Teide of the Instituto de Astrofisica de Canarias.

References

Caccin, B., Gomez, M. T., Marmolino, C., & Severino, G. 1977, A&A, 54, 227

Caccin, B., Penza, V., & Gomez, M. T. 2002, A&A, 386, 286

Cavallini, F. 1998, A&AS, 125, 589

Chapman, G. A., Herzog, A. D., & Lawrence, J. K. 1986, Nature, 319, 654

Fontenla, J. M., White, O. R., Fox, A. P., Avrett, E. H., & Kurucz, R. L. 1999, ApJ, 518, 480

Fontenla, J. M., Harder, J., Rottman, G., et al. 2004, ApJ, 605, L85

Foukal, P., & Lean, J. 1986, ApJ, 302, 826

Foukal, P., & Lean, J. 1988, APJ, 328, 347

Frölich, C. 1994, in The Sun as a Variable Star, ed. J. M. Pap, C. Frölich, H. S. Hudson, & S. K. Solanki, IAU Coll., 143, 28

Gray, D. F. 1992, The Observation and Analysis of Stellar Photospheres (Cambridge University Press)

Gray, D. F., & Johanson, H. J. 1991, PASP, 103, 439

Gray, D. F., & Livingston, W. C. 1997a, ApJ, 474, 798

Gray, D. F., & Livingston, W. C. 1997b, ApJ, 474, 802

Gray, D. F., & Livingston, W. C. 1997c, ApJ, 484, 511

Gray, R. 0. 1994, AJ, 107, 742

Hoyt, D. V., Kyle, H. L., Hickey, J. R., & Maschhoff, R. H., 1992, J. Geophys. Res., 97, 51

Kurucz, R. L., Furenlid, I., Branult, J., & Testerman, L. 1985, Sky and Telescope, 70, 38

Krivova, N. A., Solanki, S. K., Fligge, M., & Unruh, Y. C. 2003, A&A, 399, L1

Kurucz, R. L. 1994, CD-ROM No. 19

Lydon, T. J., Gunther, D. B., & Sofia, S. 1996, ApJ, 456, L127

Livingston, W., Milkey, R., & Slaughter, C. 1977, ApJ, 211, 281

Livingston, W., & Wallace, L. 2003, Sol. Phys., 212, 227

Penza, V., Caccin, B., Ermolli, I., Centrone, M., & Gomez, M. T. 2003, ESA SP-535 (Noordwijk ESA Publications Division), 299

Penza, V., Caccin, B., Ermolli, I., & Centrone, M. 2004, A&A, 413, 1115

Sofia, S., Oster, L., & Schatten, K. 1982, Sol. Phys., 80, 87

Ulrich, R. K., & Bertello, L. 1995, Nature, 377, 6546

Unruh, Y. C., Solanki, S. K., & Fligge, M. 1999, A&A, 345, 635

Willson, R. C., Gulkis, S., Janssen, M., Hudson, H. S., & Chapman, G. A. 1981, Science, 211, 700

Willson, R. C., & Hudson, H. S. 1991, Nature, 351, 42